1 **Peroxymonosulfate/solar radiation process for the removal of aqueous**

2 **microcontaminants. Kinetic modeling, influence of variables and matrix**

3 **constituents**

4 Rafael R. Solís[1,*], F. Javier Rivas[2,3,*], Ana M. Chávez[2,3], Dionysios D. Dionysiou[1]

5 [1]Environmental Engineering and Science program, Department of Chemical and

6 Environmental Engineering, University of Cincinnati, Cincinnati OH 45221-0012 (USA)

7 [2]Department of Chemical Engineering and Physical Chemistry, University of

8 Extremadura, Avda. Elvas 06006 Badajoz (Spain)

9 [3]University Institute of Water, Climate Change and Sustainability (IACYS), University

10 of Extremadura, Avda. de la Investigación 06006 Badajoz (Spain)

11 *Correspondence to Rafael Rodríguez Solís (rafarsolis@gmail.com) and F. Javier Rivas

12 (fjrivas@unex.es)

13 **Abstract**

14 New technologies to address the presence of pharmaceutical and personal care

15 products (PPCPs) in wastewater are needed, especially in those cases in which water will

16 be reused. In this work, the activation of peroxymonosulfate (PMS) with simulated solar

17 radiation has been applied to the oxidation of a mixture of six PPCPs, *i.e.* caffeine,

18 primidone, N,N-diethyl-3-methylbenzamide (DEET), methylparaben, clofibric acid and

19 ibuprofen. The sole application of solar radiation, i.e. solar photolysis, only led to the

20 oxidation of clofibric acid (complete degradation in 90 min). The combination of PMS

21 and solar radiation resulted in the degradation of all target micropollutants. The complete

22 degradation of this mixture at initial 100 ppb was achieved with 0.5 mM of initial PMS

23 after 90 min. A kinetic study that acceptably simulates the experimental data under

24 different conditions has been proposed. The effects of initial PPCP concentration (1 mg

25 L^{-1}-100 µg L^{-1}), PMS dose (0.1-5 mM), and pH (3-9) were tested and kinetically

26 simulated. Finally, the PPCPs removal study was carried out in two real water matrices

27 (river and a secondary effluent of an urban wastewater treatment plant). A higher dose of

28 PMS, ten times higher, was required to achieve complete degradation of the

29 micropollutants if compared to ultrapure water.

30 **Keywords:** Oxidation process, Peroxymonosulfate, Simulated solar radiation, PPCPs,

31 Wastewater

1. INTRODUCTION

Pharmaceuticals and personal care products (PPCPs) include a large class of chemical compounds that can be generated from anthropogenic usage, excretions and veterinary applications. The increasing concern of potential threats caused by the widespread occurrence of these chemicals in the environment has forced the assessment of efficient strategies to eliminate/reduce the presence of PPCPs (Kümmerer et al., 2018). No accepted standards to complete environmental risk assessments are available. Subsequently, substantial research is recommended to address the fate and occurrence of these compounds in the environment (Svalova, 2018). Recently, technologies based on the production of sulfate radicals are gaining more attention. Formation of these powerful oxidizing agents is commonly related to the use of persulfate or peroxymonopersulfate and further activation by radiation, catalysts and/or heat (Guerra-Rodríguez et al., 2018; Wacławek et al., 2017; Wang and Wang, 2018). The use of solar radiation contributes to minimize the energy consumption and therefore the environmental impact if compared to other irradiation systems based on UV lamps. Consequently, solar radiation is gaining attention in the water treatment field and diverse applications involving sulfate radical and solar light have been recently reported (Ferreira et al., 2020; Solís et al., 2019; Vela et al., 2019).

Six model PPCPs have been selected in this study mainly based on their occurrence in surface and wastewaters, namely primidone, caffeine, methylparaben, DEET, ibuprofen, and clofibric acid (Haman et al., 2015; Kuster et al., 2008; Yang et al., 2011). Some examples can be found in the recent literature on the application of sulfate radical based systems to degrade individual organic pollutants. For example, Chen et al. (Chen et al., 2017), treated ethyl and methyl parabens using activation of persulfate by heat. These authors found that both sulfate radicals and hydroxyl radicals contributed to the

degradation of the PPCPs with a negative effect exerted by pH and inorganic scavengers. Acero and coworkers investigated the elimination of DEET by UV activated persulfate (Acero et al., 2018) concluding that the maximum degradation rate was achieved at near-neutral pH and that natural organic matter (NOM) and radical scavengers inhibited the removal of contaminants. Lian and collaborators studied the abatement of 20 PPCPs, including ibuprofen, by radiation activated persulfate (Lian et al., 2017). Second-order rate constants of pollutants with radicals were obtained by competitive kinetics, highlighting the significant role played by carbonate radicals. In all cases, the efficacy of these technologies was proven. In this work, activation of peroxymonosulfate has been carried out by radiation emitted from a solar light simulator. Under these conditions, sulfate radicals and hydroxyl radicals can be generated by the disproportionation of the inorganic peroxide (Luo et al., 2015) especially due to the contribution of UV light; the quantum yield at 254 nm is 0.52 mol Einstein[-1] (Guan et al., 2011). Activation of peroxymonosulfate by solar radiation may have a number of advantages over the use of catalysts that need to be recovered after use or other more expensive methodologies such as heat or ultrasound. Solar radiation can be directly used with low cost and even concentrated by means of adequate parabolic collectors.

In addition, the simultaneous presence of contaminants may lead to interactions; increasing or decreasing the rate of degradation of individual PPCPs. In this work, the elimination of six model PPCPs has been conducted and the influence of the most important variables were assessed. A pseudo empirical mechanism has been applied to model the process. The impact of several radical scavengers has been investigated and the role played by the water matrix was also studied by using river water (Guadiana's river) and the effluent of the secondary treatment of the wastewater treatment plant (WWTP) of the city of Badajoz.

2. MATERIAL AND METHODS

2.1. Chemicals

The micropollutant standards were of analytical grade and purchased from Sigma-Aldrich®. Technical grade Oxone® ($2KHSO_5 \cdot KHSO_4 \cdot K_2SO_4$, CAS: 37222-66-5) and potassium peroxydisulfate ($K_2S_2O_8$, CAS: 7727-21-1) were used as the respective sources for PMS and PS. H_2O_2 (30%) was from Panreac®. The rest of chemicals were of analytical grade and purchased from Panreac® or Sigma Aldrich®. Ultrapure water (18.2 MΩ cm) from a Milli-Q® Integral 5 system was used for the preparation of all the stock and standard solutions. HPLC-grade acetonitrile was supplied for the chromatographic analyses.

2.2. Experimental installation and procedure

The solar photo-activation of PMS was carried out in a solar simulator reactor (Suntest CPS, 1500W, air-cooled Xe lamp) in which a glass beaker of 500 mL was located and kept under magnetic stirring. The light source consisted of 500 W m^{-2} of polychromatic radiation within 290-800 nm. Detailed information about the radiation characterization is available in previous work (Solís et al., 2019).

Tests started with the addition of 500 mL of water sample (ultrapure, river or wastewater) spiked with the mixture of the six micropollutants at an initial concentration ranging from 100 µg L^{-1} to 1 mg L^{-1} each. Afterward, a desired amount of PMS from a concentrated fresh solution (generally 0.1 M) was added and the irradiance lamp was connected for 2 hours. Samples were withdrawn at predetermined time intervals and the reaction solution was quenched by the addition of 10 µL of sodium thiosulfate 0.1 M to 1 mL of sample.

2.3. Aqueous analyses

The aqueous concentration of PPCPs was determined by Liquid Chromatography (LC) in a UFLC Shimadzu Prominence LC-AD equipped with Diode-Array detection. A mixture of acetonitrile (phase A) and acidified ultrapure water (0.1% H_3PO_4, phase B) was fed at a rate of 0.5 mL min^{-1}. The elution gradient program went from 95% A (5 min) to 95% B in 15 min, and kept thereafter for 1 min before returning to initial conditions in 5 min. The stationary phase used was a core-shell C18 Kinetex® (150 x 4.6 mm, particle size 5 µm & pore 100 Å). Different wavelength values, according to the maximum of absorbance for each compound, were used for the quantification.

2.4. Water characterization

Table 1 shows the main parameters that characterize the water collected in the Guadiana river (Badajoz, Spain) and after the biological treatment in the Waste Water Treatment Plant (WWTP). Water samples were filtered (>11 µm) and stored at 4 ºC before their use.

**Table 1.** Characterization of the two water matrices studied

Parameter	Guadiana river	WWTP effluent
pH	8.02 ± 0.05	7.69 ± 0.02
Conductivity (µS cm^{-1})	482.3 ± 0.6	616 ± 1
Turbidity (NTU)	1.97 ± 0.01	0.83 ± 0.01
TC (mg L^{-1})	29.06 ± 0.08	34.9 ± 0.4
IC (mg L^{-1})	12.4 ± 0.1	24.8 ± 0.4
TOC (mg L^{-1})	16.68 ± 0.05	10.12 ± 0.02
Chlorides (mg L^{-1})	60.6 ± 0.9	83 ± 11
Nitrates (mg L^{-1})	5.05 ± 0.24	16 ± 1
Phosphates (mg L^{-1})	0.14 ± 0.03	0.23 ± 0.06
Sulfates (mg L^{-1})	55 ± 1	60.4 ± 0.5

3. RESULTS AND DISCUSSION

3.1. Direct oxidation with PMS and solar photolysis

First, some control experiments were carried out to examine the role of daylight radiation or PMS to eliminate the selected target compounds. Hence, at uncontrolled pH (initial pH *ca.* 3.3) runs conducted in the presence of 1 mg L^{-1} in each PPCP using different amounts of initial PMS (from 10^{-4} to 10^{-2} M) led to the negligible conversion of contaminants after 120 min of reaction (results not shown). Next, some runs were carried out by adjusting the initial pH at 5, 7 and 9 (buffered with H_3PO_4 5 mM). Although, the presence of high concentration of phosphate could interfere in the activation of PMS (Lou et al., 2014), no significant PPCPs degradation was obtained at pH values below alkaline conditions. Actually, a low 10% conversion was obtained at pH values of 5 and 7; however, when the pH was increased to 9, the conversion of individual PPCPs increased, especially in the case of methylparaben. From Fig. 1, conversion values of roughly 40, 24, 100, 37, 41, and 33% after 120 min were obtained for caffeine, primidone, methylparaben, DEET, clofibric acid and ibuprofen, respectively.
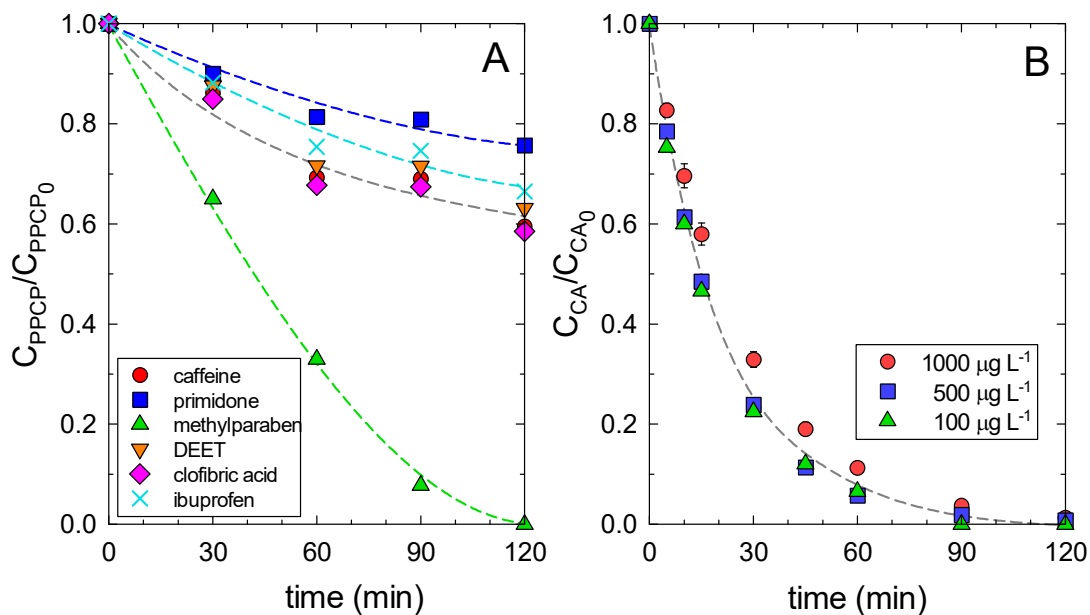
Figure 1. (A) Removal of PCPPs in water by direct oxidation by PMS at pH=9. Experimental conditions: T=293 K, $C_{PPCP,0}$=100 μg L^{-1} (each), $C_{PMS,0}$=0.5 mM, C_{H3PO4}= 5 mM; V=500 mL. (B) Removal of clofibric acid by solar photolysis. Influence of initial clofibric acid concentration. Experimental conditions: T=293 K, V=500 mL.

The efficiency increase registered at pH=9 can be attributed to the activation of peroxymonosulfate with hydroxyl anions at basic pH, releasing the generation of superoxide radical and singlet oxygen (Qi et al., 2016). Moreover, the dissociation of the target compounds can also involve a higher reactivity of the anionic form if compared to the protonated or neutral molecule. In this sense, the pK$_a$ value of methylparaben located in the proximity of 8.5 could explain the significant change in reactivity of this compound from acid-neutral conditions to pH=9. pK$_a$ values of clofibric acid (3.2), DEET (0.67) and primidone (11.5) are outside of the pH interval studied. Ibuprofen has a pK$_a$=5.3 while caffeine shows a dissociation constant of pK$_a$=10.4; however, no significant differences were obtained between pH 3.3 and 5 in the first case or between pH 7 and 9 in the second case.

Direct photolysis of PPCPs did not lead to any significant removal of target compounds with the exception of clofibric acid. The molar extinction coefficient of clofibric acid is rather low at the wavelength range of daylight radiation (Pereira et al., 2007). Nevertheless, the radiation intensity applied is enough to produce the oxidation of clofibric acid (Doll and Frimmel, 2003). It can be assumed that the removal of this compound by photolysis follows a first-order provided clofibric acid (CA) is the main absorbing species. After applying Taylor series expansion to Lambert-Beer expression:

$$-\frac{dC_{CA}}{dt} = \phi_{CA} I_o \left[1 - \exp(-2.303 L \varepsilon_{CA} C_{CA})\right] = k_{Photo} C_{CA} \tag{1}$$

where ϕ_{CA}, ε_{CA}, I_o and L stand for the quantum yield of clofibric acid, the molar extinction coefficient of clofibric acid, the incident photon flux by reactor volume unit and the effective optical path in the reactor, respectively. The experimental k_{Photo} was calculated in the proximity of $6 \cdot 10^{-4}$ s^{-1}. Experiments completed at different initial concentrations of clofibibric acid corroborated the development of first-order kinetics (see Fig. 1).

3.2. Photolysis in the presence of daylight radiation

3.2.1. Influence of initial PMS concentration

A radical mechanism can be developed when irradiating a solution of peroxymonosulfate. Under adequate irradiance conditions (wavelength and intensity), the following reactions shown in Table 2 can proceed (Guan et al., 2011; Sbardella et al., 2019; Yu and Barker, 2003).

Table 2. Mechanism of PMS irradiated system.

Reaction or equilibrium	Rate constant	Eq.
Initiation		
$HSO_5^-(aq) \xrightarrow{h\upsilon} SO_4^{\bullet-}(aq) + HO^{\bullet}(aq)$	$k_{ini1} = ?$	(2)
$SO_5^{2-}(aq) \xrightarrow{h\upsilon} SO_4^{\bullet-}(aq) + O^{\bullet-}(aq)$	$k_{ini2} = ?$	(3)
Equilibria:		

$H_2O(l) \rightleftharpoons OH^-(aq) + H^+(aq)$	$pK_w = 14$	(4)
$HOCl(aq) + HCl(aq) \rightleftharpoons Cl_2(g) + H_2O(l)$	$k = 18000\ M^{-1}\ s^{-1}$ $k_{-1} = 0.4\ M^{-1}\ s^{-1}$	(5)
$HSO_4^-(aq) \rightleftharpoons SO_4^{2-}(aq) + H^+(aq)$	$pK_a = 2$	(6)
$HSO_5^-(aq) \rightleftharpoons SO_5^{2-}(aq) + H^+(aq)$	$k = 1\ s^{-1}$ $k_{-1} = 2.5 \cdot 10^9\ M^{-1}\ s^{-1}$	(7)
$HOCl(aq) \rightleftharpoons OCl^-(aq) + H^+(aq)$	$k = 320\ s^{-1}$ $k_{-1} = 1.0 \cdot 10^{10}\ M^{-1}\ s^{-1}$	(8)

Chain reactions

$2SO_5^{\bullet-}(aq) \rightarrow 2SO_4^{\bullet-}(aq) + O_2(g)$	$k = 2.15 \cdot 10^9\ M^{-1}\ s^{-1}$	(9)
$HO^\bullet(aq) + HSO_5^-(aq) \rightarrow SO_5^{\bullet-}(aq) + H_2O(l)$	$k = 1.7 \cdot 10^7\ M^{-1}\ s^{-1}$	(10)
$S_2O_8^{2-}(aq) + H_2O(l) \rightarrow HSO_5^-(aq) + HSO_4^-(aq)$	$k = 7.5 \cdot 10^{-5}\ M^{-1}\ s^{-1}$	(11)
$SO_4^{\bullet-}(aq) + HSO_5^-(aq) \rightarrow SO_5^{\bullet-}(aq) + HSO_4^-(aq)$	$k = 1.0 \cdot 10^5\ M^{-1}\ s^{-1}$	(12)
$SO_4^{\bullet-}(aq) + H_2O(l) \rightleftharpoons HO^\bullet(aq) + HSO_4^-(aq)$	$k = 7.3\ M^{-1}\ s^{-1}$ $k_{-1} = 3.5 \cdot 10^5\ M^{-1}\ s^{-1}$	(13)
$HO^\bullet(aq) + SO_5^{2-}(aq) \rightarrow SO_5^{\bullet-}(aq) + HO^-(aq)$	$k = 2.1 \cdot 10^9\ M^{-1}\ s^{-1}$	(14)

Radical recombination:

$2HO^\bullet(aq) \rightarrow H_2O_2(aq)$	$k = 5.5 \cdot 10^9\ M^{-1}\ s^{-1}$	(15)
$2SO_4^{\bullet-}(aq) \rightarrow S_2O_8^{2-}(aq)$	$k = 3.1 \cdot 10^8\ M^{-1}\ s^{-1}$	(16)
$2SO_5^{\bullet-}(aq) \rightarrow S_2O_8^{2-}(aq) + O_2(g)$	$k = 3.5 \cdot 10^7\ M^{-1}\ s^{-1}$	(17)
$SO_4^{\bullet-}(aq) + HO^\bullet(aq) \rightarrow HSO_5^-(aq)$	$k = 1.1 \cdot 10^{10}\ M^{-1}\ s^{-1}$	(18)

Oxidation and photolysis reactions:

$PPCP(aq) + SO_4^{\bullet-}(aq) \rightarrow Intermediate(aq)$	$k = f(PPCP)$	(19)
$PPCP(aq) + HO^\bullet(aq) \rightarrow Intermediate(aq)$	$k = f(PPCP)$	(20)
$Clofibric\ acid(aq) \xrightarrow{h\upsilon} Intermediate(aq)$	$k = 6.0 \cdot 10^{-4}\ s^{-1}$ (this work)	(21)
$Scavenger / Intermediate(aq) + SO_4^{\bullet-}(aq) \rightarrow Product(aq)$	$k = f(Scavenger)$	(22)
$Scavenger / Intermediate(aq) + HO^\bullet(aq) \rightarrow Product(aq)$	$k = f(Scavenger)$	(23)

In the presence of chloride:

$Cl^-(aq) + HSO_5^-(aq) \rightarrow HClO(aq) + SO_4^{2-}(aq)$	$k = 1.87 \cdot 10^{-3}\ M^{-1}\ s^{-1}$	(24)
$Cl^-(aq) + HO^g(aq) \rightarrow HClO^{g-}(aq)$	$k = 4.3 \cdot 10^9\ M^{-1}\ s^{-1}$	(25)
$HClO^{\bullet-}(aq) \rightarrow HO^\bullet(aq) + Cl^-(aq)$	$k = 6.1 \cdot 10^9\ M^{-1}\ s^{-1}$	(26)
$HClO^\bullet(aq) + H^+(aq) \rightleftharpoons Cl^\bullet(aq) + H_2O(l)$	$k = 2.6 \cdot 10^{10}\ M^{-1}\ s^{-1}$ $k_{-1} = 3.6 \cdot 10^{10}\ M^{-1}\ s^{-1}$	(27)
$HClO(aq) + PPCP(aq) \rightarrow Intermediate(aq)$	$k = f(PPCP)$	(28)

$$Cl^{\bullet}(aq) + HSO_4^-(aq) \rightarrow HCl(aq) + SO_4^{\bullet-}(aq) \qquad k=2.5\cdot10^8 \text{ M}^{-1}\text{ s}^{-1} \qquad (29)$$

$$Cl^{\bullet}(aq) + SO_4^{2-}(aq) \rightarrow Cl^-(aq) + SO_4^{\bullet-}(aq) \qquad k=2.5\cdot10^8 \text{ M}^{-1}\text{ s}^{-1} \qquad (30)$$

$$Cl^{\bullet}(aq) + Cl^-(aq) \rightarrow Cl_2^{\bullet-}(aq) \qquad k=7.8\cdot10^9 \text{ M}^{-1}\text{ s}^{-1} \qquad (31)$$

$$Cl_2^{\bullet-}(aq) + H_2O(l) \rightarrow HClO^{\bullet}(aq) + H^+(aq) + Cl^-(aq) \qquad k\cdot C_{H2O} < 100 \text{ s}^{-1} \qquad (32)$$

$$Cl^{\bullet}(aq) + Cl_2^{\bullet-}(aq) \rightarrow Cl^-(aq) + Cl_2(g) \qquad k=2.1\cdot10^9 \text{ M}^{-1}\text{ s}^{-1} \qquad (33)$$

$$Cl_2^{\bullet-}(aq) + Cl_2^{\bullet-}(aq) \rightarrow 2Cl^-(aq) + Cl_2(g) \qquad k=9\cdot10^8 \text{ M}^{-1}\text{ s}^{-1} \qquad (34)$$

172   If the energy of the applied radiation is adequate to produce the scission of HSO_5^-

173   molecule, Eqs. 2 and 3 take place generating radical species capable of removing organic

174   and inorganic species with rate constants as high as 10^7-10^{10} M^{-1} s^{-1}.

175   Figure 2 shows the evolution of the normalized PPCPs concentrations with time in

176   experiments carried out with an initial concentration in PMS ranging from 0.1 to 5 mM.

177   As observed, the higher the initial promoter concentration, the higher the conversion rate

178   of PPCPs. Contrarily to other authors (Wu et al., 2019), experimental data indicate that,

179   under the PMS concentration used, the molecules of PMS do not react with the generated

180   radicals through reactions 10, 12, and 14. Additionally, with the exception of the

181   experiment completed with the highest PMS concentration, clofibric acid removal rate

182   seems to be independent of peroxymonosulfate dose, this compound is mainly degraded

183   by photolysis following first-order kinetics.
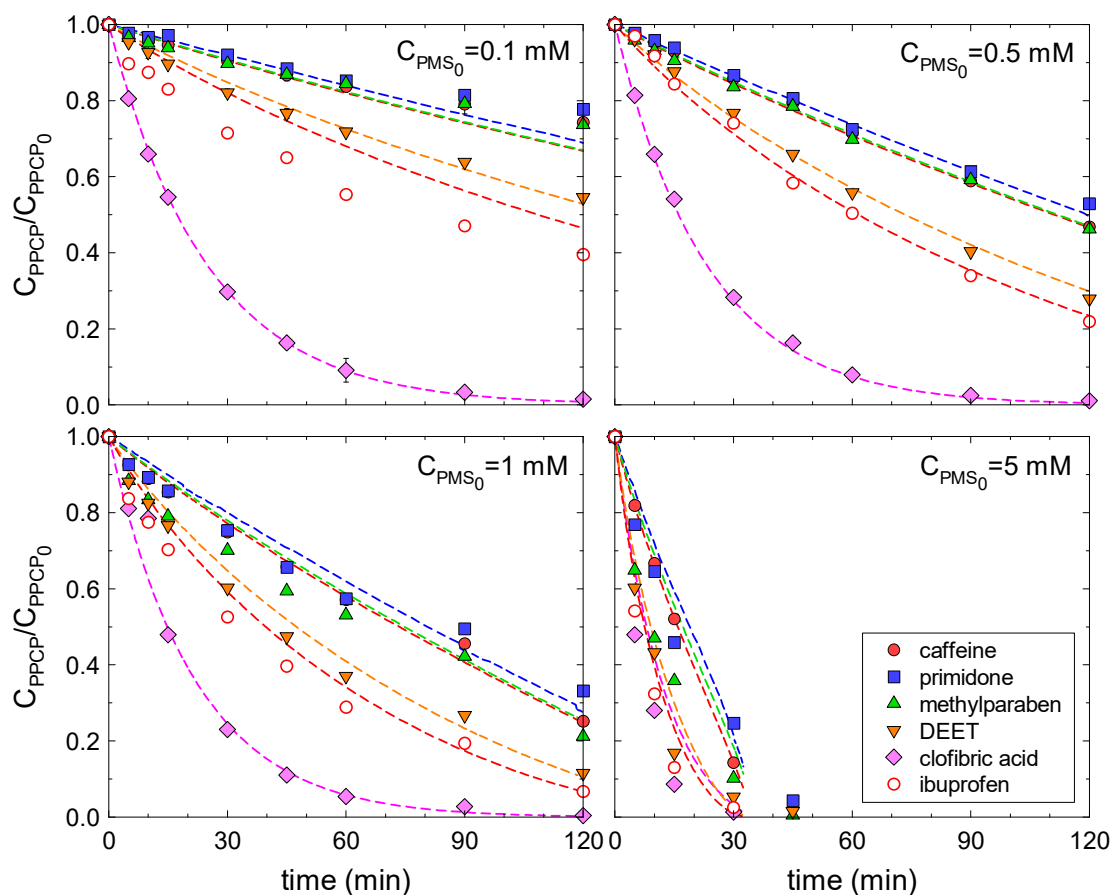
Figure 2. Removal of PPCPs in water by PMS in the presence of solar radiation. Influence of initial PMS concentration. Experimental conditions: T=293 K, $C_{PPCP,0}$=1.0 mg L^{-1} (each), V=500 mL. Lines: model calculation.

Assuming a perfectly mixed batch reactor, equations 2-23 allowed to propose a set of first-order differential equations that could be solved by adjusting the value of k_{ini1} and k_{ini2} to fit the experimental and calculated PPCPs concentrations. The software tool COPASI (Hoops et al., 2006) was used for the resolution and simulation of the generated set of ordinary differential equations. For doing so, published data of rate constants corresponding to Eqs. 19 and 20 were initially used before optimization (see Table 3). Generic values of Intermediate (P) reactions with hydroxyl radicals (5·10^9 M^{-1} s^{-1}) and sulfate radicals (5·10^9 M^{-1} s^{-1}) were assumed. Since the extinction coefficient of clofibric

acid is low and PMS remains almost constant during the experiments, the rate of PMS

photolysis can be modeled by a simple expression of the type:

$$-\frac{dC_{PMS}}{dt} = \alpha\left(C_{PMS}\right)\left(1-10^{C_{PMS}}\right) = k_{ini_1}\left(1-10^{C_{PMS}}\right) \tag{35}$$

Where the parameter $\alpha(C_{PMS})$ was experimentally observed to depend on PMS initial

concentration. The potential inefficient decomposition of peroxymonosulfate towards

sulfate and oxygen can be considered:

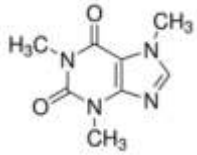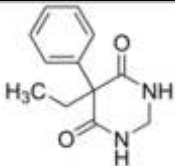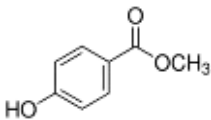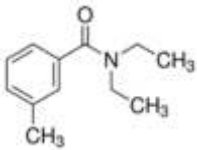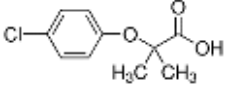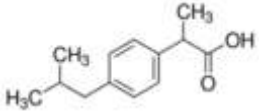$$HSO_5^- \xrightarrow{\text{Inefficient}} SO_4^{2-} + H^+ + \frac{1}{2}O_2 \tag{36}$$
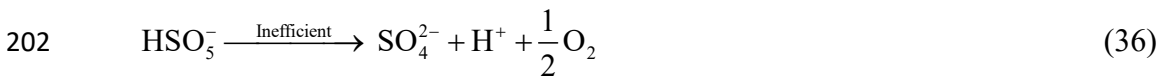
Fitted values of $\alpha(C_{PMS})$ were $5\cdot10^{-6}$, $1.7\cdot10^{-6}$, $1.3\cdot10^{-6}$, and $1.3\cdot10^{-6}$ in experiments with

PMS initial concentration of 0.1, 0.5, 1.0 and 5.0 mM, respectively. The dependency of

$\alpha(C_{PMS})$ on $C_{PMS,0}$ seems to be inversely proportional (a, b, and c are constant parameters):

$$\alpha(C_{PMS}) \propto \frac{a}{b+c\times C_{PMS_0}} \tag{37}$$

At the sight of the calculated radical concentrations, hydroxyl radical concentration is

two orders of magnitude higher than that of sulfate radicals. The reactivity of the PPCPs

studied follow the order primidone < methylparaben = caffeine < DEET < ibuprofen <

clofibric acid. These profiles could be obtained by using the second-order rate constants

for $HO^\bullet$ and $SO_4^{\bullet-}$ shown in Table 3. In general, the rate constants used with sulfate

radicals are slightly higher than those found in the bibliography.

Table 3. Physicochemical characteristics of the target pollutants used in this study and their reactivity towards $HO^{\bullet}$ and $SO_4^{\bullet-}$

PPCPs (use)	Molecular structure	Molecular formula	Water Solubility (mg L^{-1})[1]	pK$_a$[1]	Second-order rate constant with $HO^{\bullet}$ and $SO_4^{\bullet-}$					
					$k_{HO^{\bullet}} \cdot 10^{-9}$ (M^{-1} s^{-1})	pH	Ref.	$k_{SO_4^{\bullet-}} \cdot 10^{-9}$ (M^{-1} s^{-1})	pH	Ref.
Caffeine (nervous stimulant)		C$_8$H$_{10}$N$_4$O$_2$	2.16·10^4	10.4	4.1	7.0	(Shu et al., 2013)	2.39	7.0	(Nihemaiti et al., 2018)
					5.9	NA	(Broséus et al., 2009)			
					6.4±0.7	5.5-9.0	(Wols and Hofman-Caris, 2012)			
					6.9	NA	(Kesavan and Powers, 1985)			
					6.0	3.3-9.0	*this study*[2]	1.5	3.3-9.0	*this study*[2]
Primidone (drug, anticonvulsant)		C$_{12}$H$_{14}$N$_2$O$_2$	500	11.5	6.7	3.0	(Real et al., 2009)	0.53	7.0	(Nihemaiti et al., 2018)
					6.7	3.3-9.0	*this study*[2]	0.90	3.3-9.0	*this study*[2]
Methylparaben (preservative, anti-fungal)		C$_8$H$_8$O$_3$	2500	8.5	6.8	3.0	(Tay et al., 2010)		Not available	
					7.1	3.3-9.0	*this study*[2]	1.0	3.3-9.0	*this study*[2]
DEET (Insecticide, repellent)		C$_{12}$H$_{17}$NO	912	0.67	4.95	7.0	(Song et al., 2009)	9.5	7.0	(Acero et al., 2018)
					7.51	3.0	(Benitez et al., 2013)			
					8.5	3.0	(Tay et al., 2011)			
					6.0	3.3-9.0	*this study*[2]	4.0	3.3-9.0	*this study*[2]

Name	Structure	Formula					Reference			Reference
Clofibric acid (herbicide and drug, fat regulator)		$C_{10}H_{11}ClO_3$	583	3.2	4.7	3.5	(Packer et al., 2003)	1.73	7.0	(Lu et al., 2018)
					5.0±2.4	5.5-9.0	(Wols and Hofman-Caris, 2012)			
					8.0	3.3-9.0	*this study[2]*	1.7	3.3-9.0	*this study[2]*
Ibuprofen (drug, anti-inflammatory)		$C_{13}H_{18}O_2$	21	5.3	6.5	3.5	(Packer et al., 2003)	1.26	7.5	(Su et al., 2018)
					7.0±0.5	5.5-9.0	(Wols and Hofman-Caris, 2012)	1.32	7.0	(Kwon et al., 2015)
					7.4	7.0	(Marc M. Huber et al., 2003)	1.66	3.0	(Yang et al., 2017)
					7.0	3.3-9.0	*this study[2]*	4.9	3.3-9.0	*this study[2]*

214   [1]National Center for Biotechnology Information. PubChem Database

215   [2]Optimized values used in the simulation of this work

216 *3.2.2. Influence of initial PPCPs concentration*

217 An additional experimental series was carried out by changing the initial concentration

218 in each target contaminant from 100 μg L^{-1} to 1000 μg L^{-1}. Fig. 3 shows the results

219 obtained.

220 As observed, conversion rates increase as the initial concentration of contaminants is

221 decreased. The mechanism of reactions was used to simulate the results, however, the

222 value of k_{ini1} changed as the initial concentration of contaminants was varied. Hence

223 values of $1.7 \cdot 10^{-6}$ s^{-1}, $1.1 \cdot 10^{-6}$ s^{-1}, and $0.6 \cdot 10^{-6}$ s^{-1} were obtained for initial concentrations

224 of 1000, 500 and 100 μg L^{-1} of PPCPs. The reason is unclear, although clofibric acid can

225 act as a photosensitizer. Homolytic scission of a covalent bond can generate radical

226 species, such as HO$^\bullet$ and HO$_2^\bullet$ radicals or even chlorine radicals. Also, by energy transfer

227 or hydrogen abstraction, excited molecules can contribute to the abatement of aqueous

228 contaminants by the production of singlet oxygen as it is the case of pyrene used as a

229 photosensitizer (Miyoshi and Tomita, 1978). In this sense, clofibric acid was also shown

230 to photosensitize the lysis of human erythrocytes (Vargas et al., 1993). The dependency

231 of k_{ini1} with clofibric acid initial concentration was evaluated leading to a linear

232 relationship. Based on the previous results, the following expression ($R^2 > 0.99$) was

233 proposed to calculate the photolysis of PMS to generate radicals (verified under the

234 operating conditions investigated):

235
$$-\frac{dC_{PMS}}{dt} = \left[\frac{C_{CA_o}(ppb) - 600}{1.89 \times 10^{12} C_{PMS_o}(M) - 8.41 \times 10^7} + 1.2 \times 10^6 \right] \left(1 - 10^{C_{PMS}(M)} \right) \qquad (38)$$

236 However, the previous expression was only validated in the range of the operating
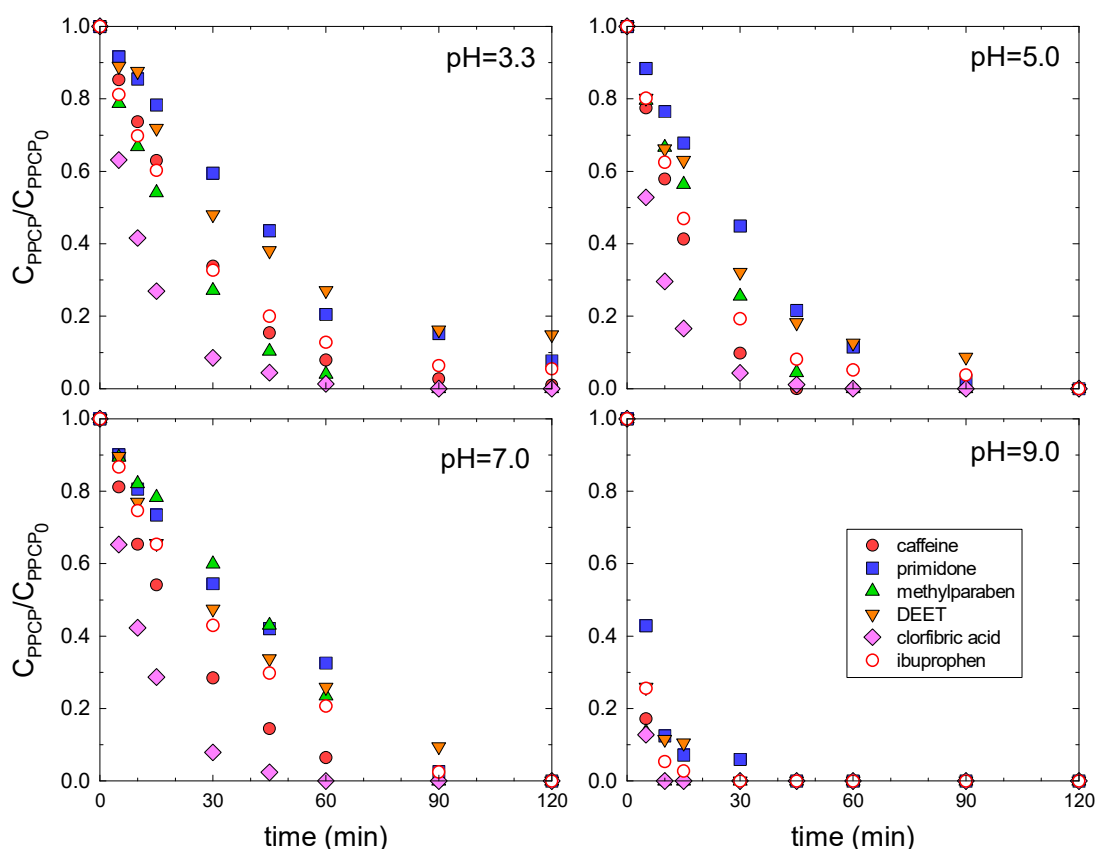
237 conditions selected.
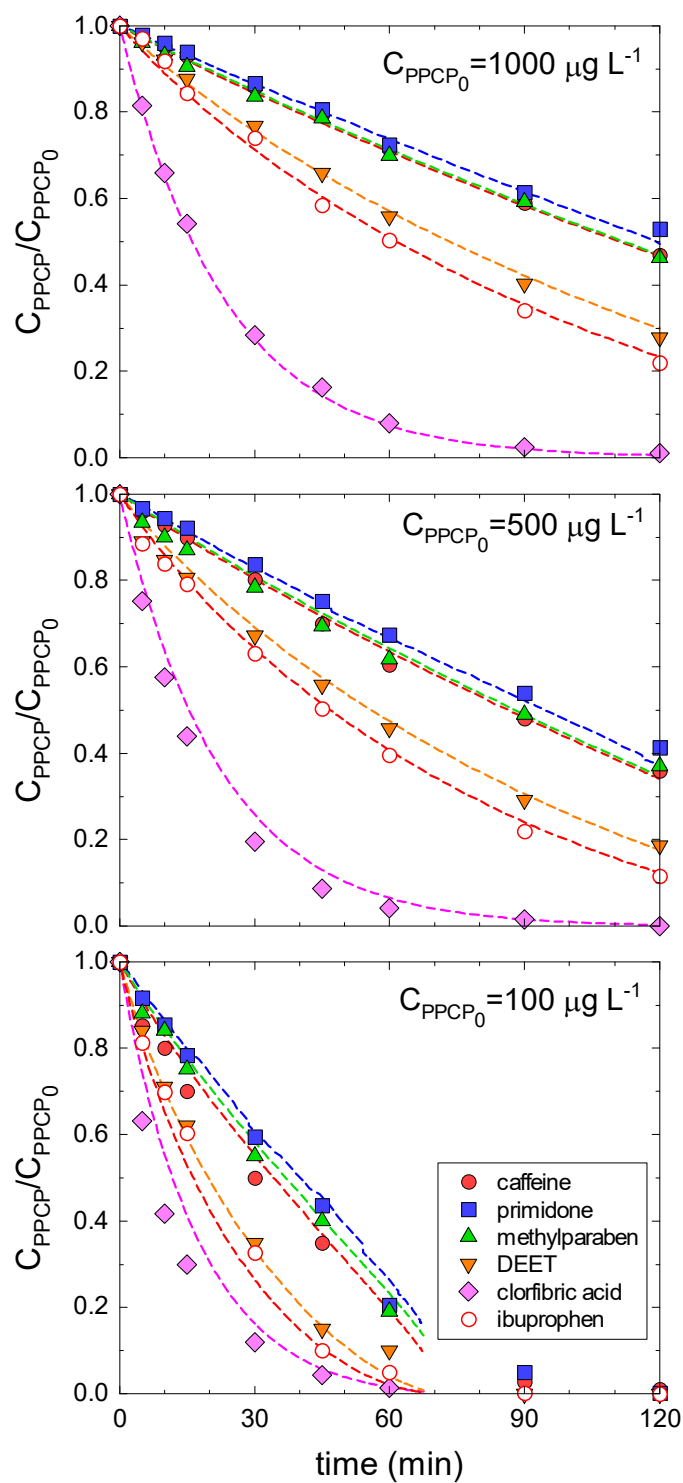
Figure 3. Removal of PPCPs in water by PMS in the presence of solar radiation. Influence of initial PPCPs concentration. Experimental conditions: $T=293$ K, $C_{PMS,0}=0.5$ mM, $V=500$ mL. Lines: model calculations.

242   *3.2.3. Influence of initial pH*

243   The influence of pH was investigated with the addition of H_3PO_4 buffer (5 mM).

244   Experiments were completed at pH values of 3.3 (no pH adjustment), 5, 7 and 9. Fig. 4

245   shows the influence of pH in which the significant impact on conversion under basic

246   conditions has to be highlighted.

247

248   **Figure 4.** Removal of PPCPs in water by PMS in the presence of solar radiation at

249   different pH values. Experimental conditions: T=293 K, $C_{PMS,0}$=0.5 mM, V=500 mL,

250    $C_{PPCP,0}$=100 µg L^{-1} (each); buffered with H_3PO_3 5 mM (pH=3.3, unbuffered).

251   This enhancement of the process at pH=9 can be justified based on (1) the higher

252   reactivity of methylparaben with PMS in the absence of radiation at alkaline pH, (2) the

253   conversion of sulfate radicals to the less selective hydroxyl radicals, (3) the potential

254   higher photoreactivity of clofibric acid (pK_a=3.2) at basic pH leading to singlet oxygen

255   generation, (4) a change of reactivity in the formula of PPCPs due to dissociation with

18

256 pH and (5) the higher radical generation by PMS photolysis. A change in reactivity of the

257 PPCPs dissociated and non-dissociated formulas are discharged as the main reason since

258 the marginal change of the second order rate constant with hydroxyl radical, see Table 3,

259 do not explain the higher reactivity registered at basic pH. However, the higher photolysis

260 of PMS at high pH was hypothesized by Guan and coworkers in the pH range 8-10 by

261 using UVC radiation (Guan et al., 2011). The apparent-molar absorption coefficient of

262 PMS is 1 order magnitude higher at pH=11 if compared to neutral pH. This behavior

263 would explain the increase of the removal rate when raising the pH from 7 to 9.

264 *3.2.4. Influence of scavengers*

265 <u>Influence of azide addition</u>

266 Previously, the potential generation of singlet oxygen was proposed as an alternative

267 route of contaminant abatement. NaN_3 is known to scavenge singlet oxygen (Xu et al.,

268 2008), however, this compound can also react with hydroxyl radical, sulfate radical and

269 even PMS. The azide ion reacts with $HO^\bullet$ with a high rate constant value of $1\text{-}8\cdot10^{10}$ M^{-1}

270 s^{-1} (Shinohara et al., 1962; Xu et al., 2008) and also with $SO_4^{\bullet-}$ but with a one magnitude

271 lower rate constant, $2.4\cdot10^9$ M^{-1} s^{-1} (Huie and Clifton, 1990). The presence of 10 mM of

272 azide completely inhibited the abatement of PPCPs with the exception of clofibric acid

273 which is eliminated by direct photolysis (results not shown). The process was simulated

274 by means of the proposed mechanism. Two strategies were adopted, first assuming that

275 azide does not react with sulfate radicals, and, secondly, assigning a rate constant of

276 $2.4\cdot10^9$ M^{-1} s^{-1} to the aforementioned reaction. In the first case, the abatement of PPCPs

277 was not inhibited, suggesting the existence of additional routes of elimination of

278 contaminants, likely due to their reaction with singlet oxygen, or alternatively, due to their

279 reaction with sulfate radicals. In the second case, PCPPs conversion modelling came to a

280 halt. As a consequence, addition of azide cannot be taken as an irrefutable proof of the

281　role played by singlet oxygen. Likely, the reaction of NaN$_3$ with sulfate radicals is the

282　reason of the complete inhibition of the oxidation process.

283　<u>Influence of t-BuOH addition</u>

284　　t-BuOH shows a relatively high reactivity towards hydroxyl radicals (3.8-7.6·10^8 M^{-1}

285　s^{-1}) and low rate constant with sulfate radicals (4.0-9.1·10^5 M^{-1} s^{-1}). Experimental results

286　indicate that in the presence of 10 mM of t-BuOH, partial inhibition of the process was

287　experienced, suggesting the presence of hydroxyl radicals in the process (Fig. 5). The

288　mechanism of reactions proposed could adequately model the kinetics of degradation for

289　the rest of the target contaminants

290　<u>Influence of EtOH addition</u>

291　　Ethanol can scavenge both hydroxyl radicals (1.2-2.8·10^9 M^{-1} s^{-1}) and sulfate radicals

292　(1.6-7.7·10^7 M^{-1} s^{-1}) if a high concentration of the scavenger is used. According to the

293　mechanism of reactions proposed, a concentration of 10 mM in ethanol should almost

294　completely inhibit PPCPs removal with the exception of clofibric acid. The lack of

295　influence of alcohols in the degradation of clofibric acid denotes, once again, that this

296　compound is not removed by the action of radicals. However, experimental data revealed

297　the partial abatement of the rest of contaminants with the exception of ibuprofen (Fig. 5).

298　From the analysis of the evolution of ibuprofen in the presence of alcohols can be

299　observed that the degradation of this PPCPs is not completely, as expected with EtOH, of

300　partially, as expected with T-BuOH, which provides some evidence of extra degradation

301　routes. These results can be explained by the presence of singlet oxygen, or even, by

302　considering that ethanol attack can initiate a radical mechanism involving the generation

303　of hydroperoxyl radicals and ultimately hydrogen peroxide according to Table 4 (Bothe

304　et al., 1983).

305 **Table 4**. PMS photolysis mechanism: scavenging reactions in the presence of EtOH

Reaction	Rate constant	Eq.
$CH_3CH_2OH(aq) + HO^\bullet(aq) \rightarrow CH_3CHOH^\bullet(aq) + H_2O(l)$	$k=1.2\text{-}2.8\cdot10^9 \text{ M}^{-1}\text{ s}^{-1}$	(39)
$CH_3CH_2OH(aq) + SO_4^{\bullet-}(aq) \rightarrow CH_3CHOH^\bullet(aq) + H_2O(l)$	$1.6\text{-}7.7\cdot10^7 \text{ M}^{-1}\text{ s}^{-1}$	(40)
$CH_3CHOH^\bullet(aq) + O_2(g) \rightarrow CH_3CO_2HOH^\bullet(aq)$	$k=3.5\cdot10^8 \text{ M}^{-1}\text{ s}^{-1}$	(41)
$CH_3CO_2HOH^\bullet(aq) \rightarrow CH_3CHO(aq) + HO_2^\bullet(aq)$	$k=9\cdot10^7 \text{ s}^{-1}$	(42)
$CH_3CO_2HOH^\bullet(aq) \rightarrow CH_3CHO(aq) + O_2^{\bullet-}(aq)$	$k=4\cdot10^9 \text{ s}^{-1}$	(43)
$2\,CH_3CO_2HOH^\bullet(aq) \rightarrow CH_3CHOH-OOOO-HOHCH_3C(aq)$	$k=3.5\cdot10^8 \text{ M}^{-1}\text{ s}^{-1}$	(44)
$CH_3CHOH-OOOO-HOHCH_3C(aq) \rightarrow 2CH_3COHOH^\bullet(aq) + O_2(g)$	Not available	(45)
$CH_3CHOH-OOOO-HOHCH_3C(aq) \rightarrow 2CH_3COHOH^\bullet(aq) + H_2O_2(aq)$	Not available	(46)
$2CH_3COHOH^\bullet(aq) \rightarrow \begin{cases} 2HO_2^\bullet(aq) + 2CH_3COOH(aq) \\ 2CH_3^\bullet(aq) + 2HCOOH(aq) \end{cases}$	Not available	(47)
$HO_2^\bullet(aq) + O_2^{\bullet-}(aq) + H^+(aq) \rightarrow H_2O_2(aq) + O_2(g)$	$k=9.0\cdot10^7$	(48)

306 Hydrogen peroxide generated in the previous mechanism can undergo homolytic

307 scission by radiation to form hydroxyl radicals. Alternatively, some compounds can react

308 with hydroperoxyl radical or methyl radical.
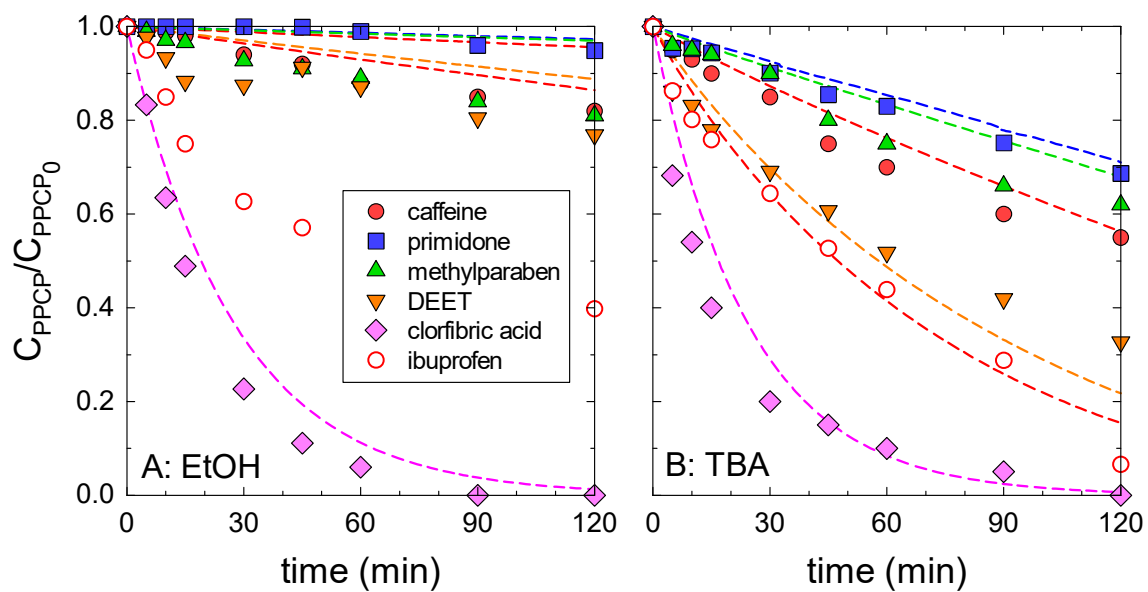
Figure 5. Removal of PPCPs in water by PMS in the presence of solar radiation. Influence of the scavenging effect of ethanol (A) and TBA (B). Experimental conditions: T=293 K, $C_{PMS,0}$=0.5 mM, V=500 mL, $C_{PPCP,0}$=100 µg L^{-1} (each); $C_{scavenger}$=10 mM; pH=unbuffered. Lines: model calculations.

3.3. PMS photolysis in real water matrices

Real waters present a variety of substances capable of inhibiting the radicals present in the system. The main species to be considered are the organic matter (measured as total organic carbon, TOC), carbonate (measured as inorganic carbon, IC), nitrate, sulfate and chloride. Accordingly, the reactions summarized in Table 5 should be added to the general mechanism (Ahn et al., 2017; Lee et al., 2020; Lian et al., 2017).

Table 5. PMS photolysis mechanism: scavenging reactions in real water matrix

Reaction	Rate constant (M^{-1} s^{-1})	Eq.
$HO^{\bullet}(aq) + CO_3^{2-}(aq) \rightarrow CO_3^{\bullet-}(aq) + H_2O(l)$	$k = 3.9 \cdot 10^8$	(49)
$HO^{\bullet}(aq) + HCO_3^{-}(aq) \rightarrow CO_3^{\bullet-}(aq) + HO^{-}(aq)$	$k = 8.6 \cdot 10^6$	(50)
$SO_4^{\bullet-}(aq) + HCO_3^{-}(aq) \rightarrow CO_3^{\bullet-}(aq) + HSO_4^{-}(aq)$	$k = 2.8 \cdot 10^6$	(51)
$SO_4^{\bullet-}(aq) + CO_3^{2-}(aq) \rightarrow CO_3^{\bullet-}(aq) + SO_4^{2-}(aq)$	$k = 6.1 \cdot 10^6$	(52)
$SO_4^{\bullet-}(aq) + Cl^{-}(aq) \rightarrow Cl^{\bullet}(aq) + SO_4^{2-}(aq)$	$k = 3.0 \cdot 10^8$	(53)
$HO^{\bullet}(aq) + TOC(aq) \rightarrow P(aq)$	$k = (1.6\text{-}3.3) \cdot 10^8$	(54)
$SO_4^{\bullet-}(aq) + TOC(aq) \rightarrow P(aq)$	$k = (2.5\text{-}8.1) \cdot 10^7$	(55)
$SO_4^{\bullet-}(aq) + NO_3^{-}(aq) \rightarrow NO_3^{\bullet}(aq) + SO_4^{2-}(aq)$	$k = 2.1 \cdot 10^6$	(56)

An experimental series was carried out with water taken from the Guadiana River in Badajoz after spiking with 100 µg L^{-1} in each pharmaceutical. As observed in Fig. 6, with the exception of clofibric acid, the degradation rate for the rest of pharmaceuticals significantly decreased if compared to the run completed performed in ultrapure water (Fig. 2). Degradation percentages after 2 hours also decreased. Competition for radicals seems to be the reason for this effect. Common values for the reaction of radicals with organic matter (Eqs. 54 and 55) allowed to simulate the process and predict the experimental kinetics with a low error. Several studies report that the second order rate

329   constant between natural organic matter and sulfate radicals are 1 magnitude lower than

330   the respective with hydroxyl radical (Lee et al., 2020).

331   According to the previous results, an increase in radical generation is suggested to

332   enhance the removal rate of target contaminants. Consequently, an experimental series

333   was carried out by increasing the amount of PMS added at the beginning. Fig. 6 shows

334   the beneficial effect of higher doses of peroxymonosulfate.
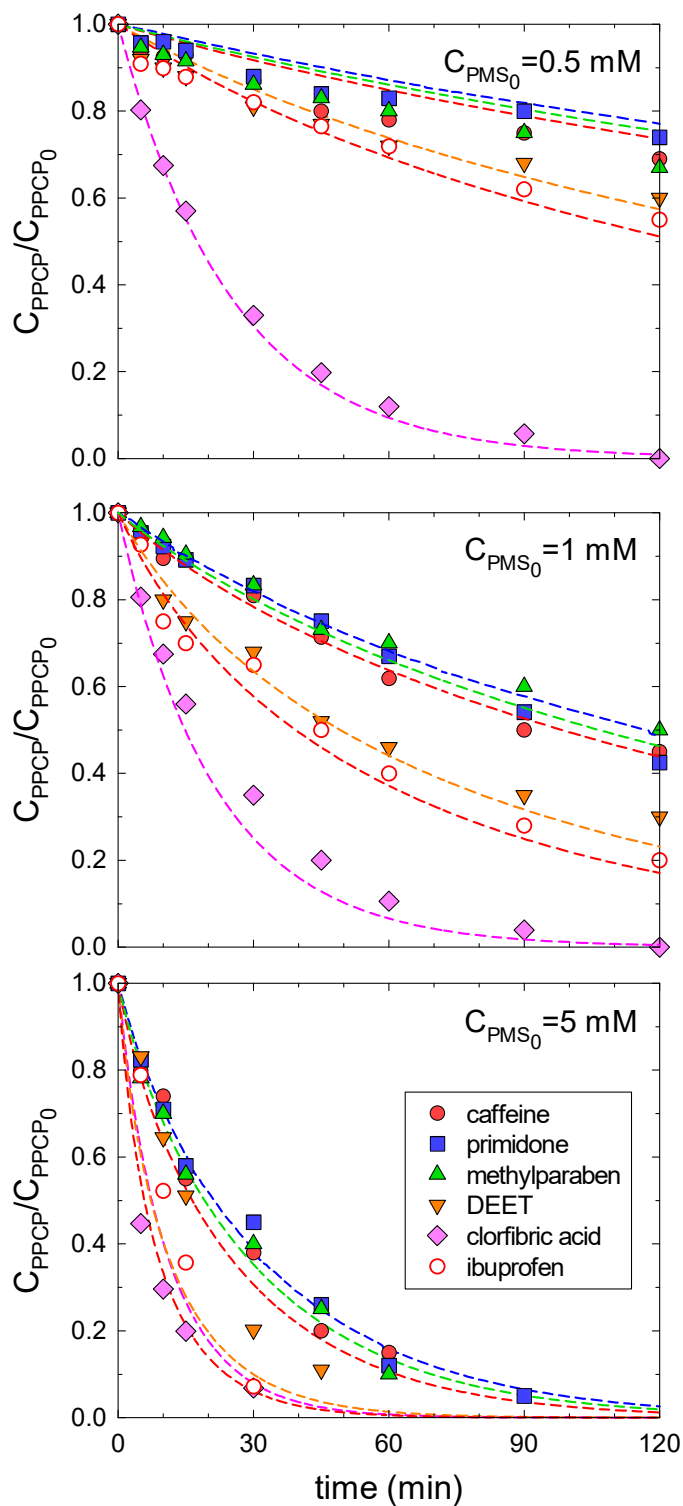
Figure 6. Removal of PPCPs in Guadiana River water by PMS in the presence of solar radiation. Influence of initial PMS concentration. Experimental conditions: T=293 K, V=500 mL, $C_{PPCP,0}$=100 µg L^{-1} (each). Lines: model calculation.

A similar experimental series was carried out by spiking the wastewater effluent of a wastewater treatment plant. The role of PMS dose was tested also in the range 0.5-5 mM.

25

341   All the micropollutants were satisfactorily oxidized after 120 min with an initial PMS

342   dose of 5 mM. As observed in Fig. 7, this effluent presented a higher scavenging capacity

343   of radicals, inhibiting the process to a higher extent under similar conditions than that

344   used with river water. The WWTP effluent presented lower TOC value than the river

345   water; therefore, the higher amount of inorganic carbon and chloride may explain the

346   greater scavenging effect observed in the WWTP effluent. If the application of the model

347   is analyzed for both matrices, the model prediction is more accurate for the river effluent.

348   In the WWTP matrix, the model underestimates the scavenging effect of the matrix. A

349   plausible explanation for that effect may be the different nature of the organic matter

350   between the two matrices. Substances accounting for TOC in WWTP are more reactive

351   than what is considered in Eqs. 54 and 55 and the standard value considered for the kinetic

352   rate constant is not representative of the TOC of this matrix.

353   The treatment of wastewater with inorganic peroxides such as peroxymonosulfate

354   results in an increase of sulfates in water after treatment. Considering that all the sulfur

355   contained in PMS is transformed into sulfate, and also the sulfate already included in

356   Oxone® salt formula, a final amount of 480 mg L^{-1} of sulfate would be added to the initial

357   55 and 60.4 mg L^{-1} already present in the river and wastewater matrices, respectively.

358   Depending on the further application or discharge policy, sulfate may need additional

359   removal from water.
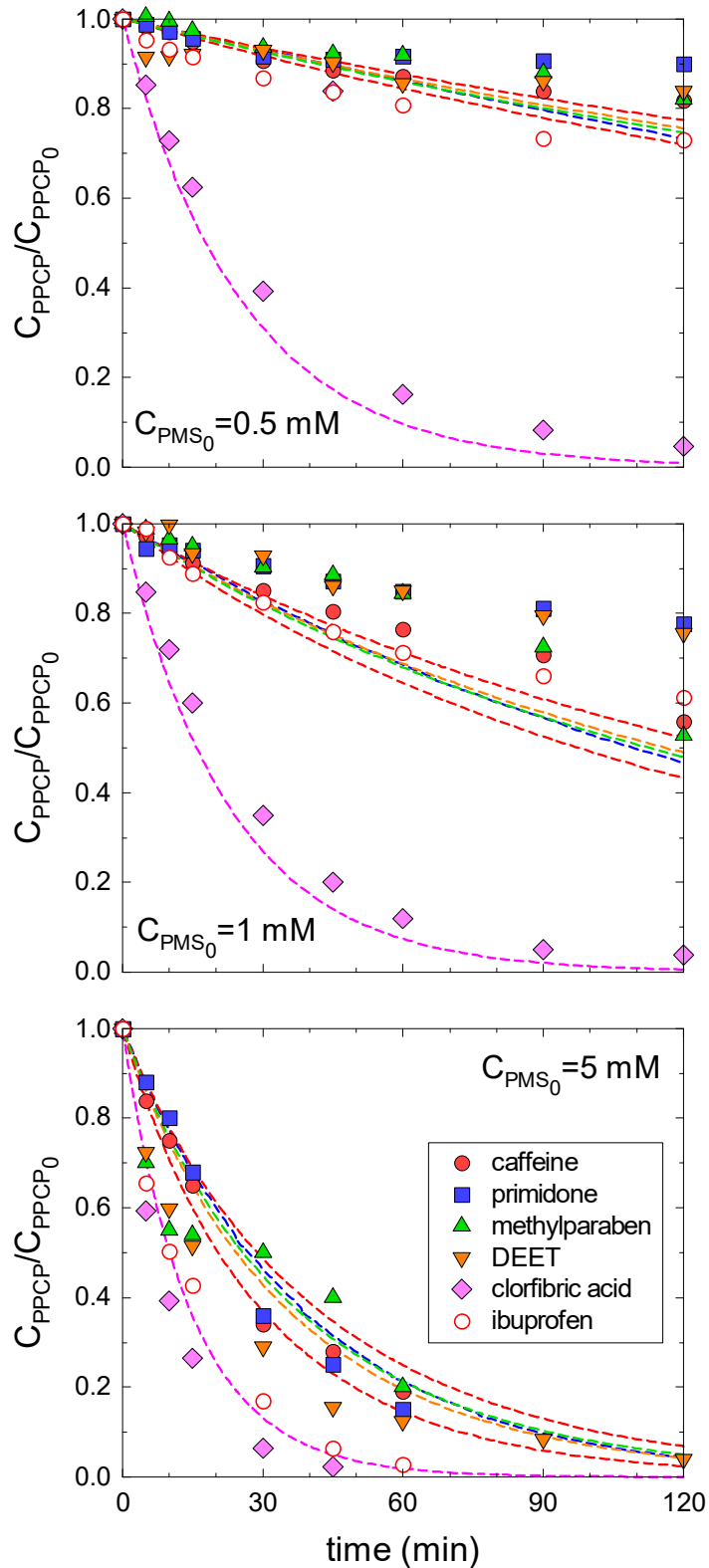
Figure 7. Removal of PPCPs in WWTP effluent by PMS in the presence of solar radiation. Influence of initial PMS concentration. Experimental conditions: T=293 K, V=500 mL $C_{PPCP,0}$=100 µg L^{-1} (each). Lines: model calculation.

4. CONCLUSIONS

A mixture of six organic micropollutants representative of the typical pharmaceutical and personal care products (i.e. caffeine, primidone, methylparaben, DEET, clofibric acid and ibuprofen) detected in aqueous effluents has been successfully treated by the combination of peroxymonosulfate and solar radiation. The irradiation of PMS leads to the generation of hydroxyl radicals and sulfate radicals, as scavenging test suggested, capable of oxidizing the organic contaminants. In the absence of radiation, no direct oxidation of the contaminants was observed except for methylparaben at a basic pH. Clofibric acid showed preferential oxidation by the sole action of radiation (photolysis). The reactivity of the compounds followed the order methylparaben > caffeine > ibuprofen > primidone ~ DEET.

The kinetic simulation of the whole process considering initiation, mainly the formation of hydroxyl radicals and sulfate radicals, propagation and termination steps was satisfactorily able to describe the experimental profile of the PPCPs concentration versus time. Different conditions, such as initial PMS concentration, initial PPCPs concentration, pH and matrix constituents were taken into account for proper modeling of the kinetics of the process.

387   Sustainability" and the Herman Schneider Professorship in the College of Engineering

388   and Applied Sciences.

389   **REFERENCES**

390   Acero, J.L., Benítez, F.J., Real, F.J., Rodríguez, E., 2018. Degradation of selected
391   emerging contaminants by UV-activated persulfate: Kinetics and influence of matrix
392   constituents. Sep. Purif. Technol. 201, 41–50.
393   https://doi.org/https://doi.org/10.1016/j.seppur.2018.02.055

394   Ahn, Y., Lee, D., Kwon, M., Choi, I. hwan, Nam, S.N., Kang, J.W., 2017. Characteristics
395   and fate of natural organic matter during UV oxidation processes. Chemosphere 184,
396   960–968. https://doi.org/10.1016/j.chemosphere.2017.06.079

397   Benitez, F.J., Acero, J.L., Real, F.J., Roldan, G., Rodriguez, E., 2013. Modeling the
398   photodegradation of emerging contaminants in waters by UV radiation and
399   UV/H2O2 system. J. Environ. Sci. Heal. - Part A Toxic/Hazardous Subst. Environ.
400   Eng. 48, 120–128. https://doi.org/10.1080/10934529.2012.707864

401   Bothe, E., Nien Schuchmann, M., Schulte-Frohlinde, D., von Sonntag, C., 1983.
402   Hydroxyl Radical-Induced Oxidation of Ethanol in Oxygenated Aqueous Solutions.
403   A Pulse Radiolysis and Product Study. Zeitschrift fur Naturforsch. - Sect. B J. Chem.
404   Sci. 38, 212–219. https://doi.org/10.1515/znb-1983-0218

405   Broséus, R., Vincent, S., Aboulfadl, K., Daneshvar, A., Sauvé, S., Barbeau, B., Prévost,
406   M., 2009. Ozone oxidation of pharmaceuticals, endocrine disruptors and pesticides
407   during drinking water treatment. Water Res. 43, 4707–4717.
408   https://doi.org/10.1016/j.watres.2009.07.031

409   Chen, Y., Deng, P., Xie, P., Shang, R., Wang, Z., Wang, S., 2017. Heat-activated
410   persulfate oxidation of methyl- and ethyl-parabens: Effect, kinetics, and mechanism.
411   Chemosphere 168, 1628–1636.
412   https://doi.org/https://doi.org/10.1016/j.chemosphere.2016.11.143

413   Doll, T.E., Frimmel, F.H., 2003. Fate of pharmaceuticals—photodegradation by
414   simulated solar UV-light. Chemosphere 52, 1757–1769.
415   https://doi.org/10.1016/S0045-6535(03)00446-6

416   Ferreira, L.C., Castro-Alférez, M., Nahim-Granados, S., Polo-López, M.I., Lucas, M.S.,
417   Li Puma, G., Fernández-Ibáñez, P., 2020. Inactivation of water pathogens with solar
418   photo-activated persulfate oxidation. Chem. Eng. J. 381, 122275.
419   https://doi.org/10.1016/j.cej.2019.122275

420   Guan, Y.-H., Ma, J., Li, X.-C., Fang, J.-Y., Chen, L.-W., 2011. Influence of pH on the
421   Formation of Sulfate and Hydroxyl Radicals in the UV/Peroxymonosulfate System.

Environ. Sci. Technol 45, 9308–9314. https://doi.org/10.1021/es2017363

Guerra-Rodríguez, S., Rodríguez, E., Singh, D.N., Rodríguez-Chueca, J., Guerra-Rodríguez, S., Rodríguez, E., Singh, D.N., Rodríguez-Chueca, J., Singh, N.D., Rodríguez-Chueca, J., 2018. Assessment of Sulfate Radical-Based Advanced Oxidation Processes for Water and Wastewater Treatment: A Review. Water 10, 1828. https://doi.org/10.3390/w10121828

Haman, C., Dauchy, X., Rosin, C., Munoz, J.F., 2015. Occurrence, fate and behavior of parabens in aquatic environments: A review. Water Res. https://doi.org/10.1016/j.watres.2014.09.030

Hoops, S., Gauges, R., Lee, C., Pahle, J., Simus, N., Singhal, M., Xu, L., Mendes, P., Kummer, U., 2006. COPASI - A COmplex PAthway SImulator. Bioinformatics 22, 3067–3074. https://doi.org/10.1093/bioinformatics/btl485

Huie, R.E., Clifton, C.L., 1990. Temperature dependence of the rate constants for reactions of the sulfate radical, SO4-, with anions. J. Phys. Chem. 94, 8561–8567. https://doi.org/10.1021/j100386a015

Kesavan, P.C., Powers, E.L., 1985. Differential Modification of Oxic and Anoxic Components of Radiation Damage in *Bacillus Megaterium* Spores by Caffeine. Int. J. Radiat. Biol. Relat. Stud. Physics, Chem. Med. 48, 223–233. https://doi.org/10.1080/09553008514551221

Kümmerer, K., Dionysiou, D.D., Olsson, O., Fatta-Kassinos, D., 2018. A path to clean water. Science (80-.). 361, 222–224. https://doi.org/10.1126/science.aau2405

Kuster, M., López de Alda, M.J., Hernando, M.D., Petrovic, M., Martín-Alonso, J., Barceló, D., 2008. Analysis and occurrence of pharmaceuticals, estrogens, progestogens and polar pesticides in sewage treatment plant effluents, river water and drinking water in the Llobregat river basin (Barcelona, Spain). J. Hydrol. 358, 112–123. https://doi.org/10.1016/J.JHYDROL.2008.05.030

Kwon, M., Kim, S., Yoon, Y., Jung, Y., Hwang, T.M., Lee, J., Kang, J.W., 2015. Comparative evaluation of ibuprofen removal by UV/H2O2 and UV/S2O82- processes for wastewater treatment. Chem. Eng. J. 269, 379–390. https://doi.org/10.1016/j.cej.2015.01.125

Lee, J., von Gunten, U., Kim, J.-H., 2020. Persulfate-based Advanced Oxidation: Critical Assessment of Opportunities and Roadblocks. Environ. Sci. Technol. 54, 3064–3081. https://doi.org/10.1021/acs.est.9b07082

Lian, L., Yao, B., Hou, S., Fang, J., Yan, S., Song, W., 2017. Kinetic Study of Hydroxyl and Sulfate Radical-Mediated Oxidation of Pharmaceuticals in Wastewater Effluents. Environ. Sci. Technol. 51, 2954–2962.

458   https://doi.org/10.1021/acs.est.6b05536

459   Lou, X., Wu, L., Guo, Y., Chen, C., Wang, Z., Xiao, D., Fang, C., Liu, J., Zhao, J., Lu,
460   S., 2014. Peroxymonosulfate activation by phosphate anion for organics degradation
461   in water. Chemosphere 117, 582–585.
462   https://doi.org/10.1016/j.chemosphere.2014.09.046

463   Lu, X., Shao, Y., Gao, N., Chen, J., Deng, H., Chu, W., An, N., Peng, F., 2018.
464   Investigation of clofibric acid removal by UV/persulfate and UV/chlorine processes:
465   Kinetics and formation of disinfection byproducts during subsequent
466   chloramination. Chem. Eng. J. 331, 364–371.
467   https://doi.org/10.1016/J.CEJ.2017.08.117

468   Luo, C., Ma, J., Jiang, J., Liu, Y., Song, Y., Yang, Y., Guan, Y., Wu, D., 2015. Simulation
469   and comparative study on the oxidation kinetics of atrazine by UV/H2O2,
470   UV/HSO5- and UV/S2O82-. Water Res. 80, 99–108.
471   https://doi.org/10.1016/j.watres.2015.05.019

472   Marc M. Huber, Silvio Canonica, Gun-Young Park, A., Gunten, U. von, 2003. Oxidation
473   of Pharmaceuticals during Ozonation and Advanced Oxidation Processes. Environ.
474   Sci. Technol. 37, 1016–1024. https://doi.org/10.1021/ES025896H

475   Miyoshi, N., Tomita, G., 1978. Production and Reaction of Singlet Oxygen in Aqueous
476   Micellar Solutions Using Pyrene as Photosensitizer. Zeitschrift fur Naturforsch. -
477   Sect. B J. Chem. Sci. 33, 622–627. https://doi.org/10.1515/znb-1978-0612

478   Nihemaiti, M., Miklos, D.B., Hübner, U., Linden, K.G., Drewes, J.E., Croué, J.P., 2018.
479   Removal of trace organic chemicals in wastewater effluent by UV/H2O2 and
480   UV/PDS. Water Res. 145, 487–497. https://doi.org/10.1016/j.watres.2018.08.052

481   Packer, J.L., Werner, J.J., Latch, D.E., McNeill, K., Arnold, W.A., 2003. Photochemical
482   fate of pharmaceuticals in the environment: Naproxen, diclofenac, clofibric acid, and
483   ibuprofen. Aquat. Sci. 65, 342–351. https://doi.org/10.1007/s00027-003-0671-8

484   Pereira, V.J., Linden, K.G., Weinberg, H.S., 2007. Evaluation of UV irradiation for
485   photolytic and oxidative degradation of pharmaceutical compounds in water. Water
486   Res. 41, 4413–4423. https://doi.org/https://doi.org/10.1016/j.watres.2007.05.056

487   Qi, C., Liu, X., Ma, J., Lin, C., Li, X., Zhang, H., 2016. Activation of peroxymonosulfate
488   by base: Implications for the degradation of organic pollutants. Chemosphere 151,
489   280–288. https://doi.org/10.1016/j.chemosphere.2016.02.089

490   Real, F.J., Benitez, F.J., Acero, J.L., Sagasti, J.J.P., Casas, F., 2009. Kinetics of the
491   Chemical Oxidation of the Pharmaceuticals Primidone, Ketoprofen, and Diatrizoate
492   in Ultrapure and Natural Waters. Ind. Eng. Chem. Res. 48, 3380–3388.
493   https://doi.org/10.1021/ie801762p

494 Sbardella, L., Velo-Gala, I., Comas, J., Rodríguez-Roda Layret, I., Fenu, A., Gernjak, W.,
495 2019. The impact of wastewater matrix on the degradation of pharmaceutically
496 active compounds by oxidation processes including ultraviolet radiation and sulfate
497 radicals. J. Hazard. Mater. 380, 120869.
498 https://doi.org/10.1016/j.jhazmat.2019.120869

499 Shinohara, K., Shida, T., Saito, N., 1962. Radiation Decomposition of Aqueous Azide
500 Solution. J. Chem. Phys. 37, 173–177. https://doi.org/10.1063/1.1732947

501 Shu, Z., Bolton, J.R., Belosevic, M., Gamal El Din, M., 2013. Photodegradation of
502 emerging micropollutants using the medium-pressure UV/H2O2 Advanced
503 Oxidation Process. Water Res. 47, 2881–2889.
504 https://doi.org/10.1016/j.watres.2013.02.045

505 Solís, R.R., Rivas, F.J., Chávez, A.M., Dionysiou, D.D., 2019. Simulated solar photo-
506 assisted decomposition of peroxymonosulfate. Radiation filtering and operational
507 variables influence on the oxidation of aqueous bezafibrate. Water Res. 162, 383–
508 393. https://doi.org/10.1016/j.watres.2019.06.063

509 Song, W., Cooper, W.J., Peake, B.M., Mezyk, S.P., Nickelsen, M.G., O'Shea, K.E., 2009.
510 Free-radical-induced oxidative and reductive degradation of N,N′-diethyl-m-
511 toluamide (DEET): Kinetic studies and degradation pathway. Water Res. 43, 635–
512 642. https://doi.org/10.1016/j.watres.2008.11.018

513 Su, R., Wei, Z., Luo, S., Spinney, R., Gao, L., Liu, Y., Wu, C., Chai, L., Xiao, R., 2018.
514 Environmental Matrix Effects on Degradation Kinetics of Ibuprofen in a UV/
515 Persulfate System. J. Adv. Oxid. Technol. 21.
516 https://doi.org/10.26802/jaots.2017.0067

517 Svalova, Z.H.E.-V., 2018. Pharmaceuticals and Personal Care Products: Risks,
518 Challenges, and Solutions. IntechOpen, Rijeka.
519 https://doi.org/10.5772/intechopen.70799

520 Tay, K.S., Rahman, N.A., Abas, M.R. Bin, 2011. Removal of Selected Endocrine
521 Disrupting Chemicals and Personal Care Products in Surface Waters and Secondary
522 Wastewater by Ozonation. Water Environ. Res. 83, 684–691.
523 https://doi.org/10.2175/106143011x12989211841179

524 Tay, K.S., Rahman, N.A., Abas, M.R. Bin, 2010. Ozonation of parabens in aqueous
525 solution: Kinetics and mechanism of degradation. Chemosphere 81, 1446–1453.
526 https://doi.org/10.1016/j.chemosphere.2010.09.004

527 Vargas, F., Canudas, N., Miranda, M.A., Boscá, F., 1993. In vitro phototoxicity of
528 clofibrate. Photochemical and photohemolytic studies on its metabolite clofibric
529 acid. J. Photochem. Photobiol. B Biol. 21, 61–67.
530 https://doi.org/https://doi.org/10.1016/1011-1344(93)80165-6

Vela, N., Fenoll, J., Garrido, I., Pérez-Lucas, G., Flores, P., Hellín, P., Navarro, S., 2019. Reclamation of agro-wastewater polluted with pesticide residues using sunlight activated persulfate for agricultural reuse. Sci. Total Environ. 660, 923–930. https://doi.org/10.1016/j.scitotenv.2019.01.060

Wacławek, S., Lutze, H. V., Grübel, K., Padil, V.V.T., Černík, M., Dionysiou, D.D., 2017. Chemistry of persulfates in water and wastewater treatment: A review. Chem. Eng. J. 330, 44–62. https://doi.org/10.1016/J.CEJ.2017.07.132

Wang, J., Wang, S., 2018. Activation of persulfate (PS) and peroxymonosulfate (PMS) and application for the degradation of emerging contaminants. Chem. Eng. J. 334, 1502–1517. https://doi.org/10.1016/J.CEJ.2017.11.059

Wols, B.A., Hofman-Caris, C.H.M., 2012. Review of photochemical reaction constants of organic micropollutants required for UV advanced oxidation processes in water. Water Res. https://doi.org/10.1016/j.watres.2012.03.036

Wu, Y., Fang, Z., Shi, Y., Chen, H., Liu, Y., Wang, Y., Dong, W., 2019. Activation of peroxymonosulfate by BiOCl@Fe3O4 catalyst for the degradation of atenolol: Kinetics, parameters, products and mechanism. Chemosphere 216, 248–257. https://doi.org/https://doi.org/10.1016/j.chemosphere.2018.10.012

Xu, Z., Jing, C., Li, F., Meng, X., 2008. Mechanisms of Photocatalytical Degradation of Monomethylarsonic and Dimethylarsinic Acids Using Nanocrystalline Titanium Dioxide. Environ. Sci. Technol. 42, 2349–2354. https://doi.org/10.1021/es0719677

Yang, X., Flowers, R.C., Weinberg, H.S., Singer, P.C., 2011. Occurrence and removal of pharmaceuticals and personal care products (PPCPs) in an advanced wastewater reclamation plant. Water Res. 45, 5218–5228. https://doi.org/10.1016/J.WATRES.2011.07.026

Yang, Z., Su, R., Luo, S., Spinney, R., Cai, M., Xiao, R., Wei, Z., 2017. Comparison of the reactivity of ibuprofen with sulfate and hydroxyl radicals: An experimental and theoretical study. Sci. Total Environ. 590–591, 751–760. https://doi.org/https://doi.org/10.1016/j.scitotenv.2017.03.039

Yu, X.Y., Barker, J.R., 2003. Hydrogen peroxide photolysis in acidic aqueous solutions containing chloride ions. II. Quantum yield of HÒ(Aq) radicals. J. Phys. Chem. A 107, 1325–1332. https://doi.org/10.1021/jp026666s